

# A Novel Technique for Partial Discharge and Breakdown Investigation Based on Current Pulse Waveform Analysis

**Hitoshi Okubo**

EcoTopia Science Institute, Nagoya University.  
Furo-cho, Chikusa-ku,  
Nagoya 464-8603, Japan

**Naoki Hayakawa**

Department of Electrical Engineering and Computer Science, Nagoya University.  
Furo-cho, Chikusa-ku,  
Nagoya 464-8603, Japan

## ABSTRACT

**A novel technique for partial discharge (PD) measurement and analysis (PD-CPWA: PD Current Pulse Waveform Analysis) is developed and introduced in this paper. PD-CPWA is expected to be utilized to discuss PD mechanisms and physics in electrical insulating materials, focusing on the PD current pulse waveform and its time transition from PD inception to breakdown (BD). In this paper, the concept and principle of PD-CPWA are described, and the applications of PD-CPWA to (1) epoxy spacer samples under thermal and electric combined stresses in GIS, (2) creepage PD on epoxy spacers in SF<sub>6</sub> gas and (3) liquid nitrogen / polypropylene laminated paper composite insulation system for high temperature superconducting cables are introduced and discussed.**

**Index Terms — Electrical insulation, dielectric materials, partial discharges, breakdown, current measurement, waveform analysis.**

## 1 INTRODUCTION

FOR the insulation diagnosis of electrical insulating materials in high-voltage power apparatus, partial discharge (PD) measurement has been recognized as an important tool [1]. However, physical mechanisms from PD inception to breakdown (BD) have not been well understood [2, 3]. Future PD measurement should be based on the physical mechanisms of PD inception, propagation, degradation and BD of the materials, which will contribute to the reliable insulation diagnosis of high-voltage power apparatus.

Since PD signals are so faint and have the frequency component as high as the order of GHz [4], PD measurement in electrical insulating materials is very difficult. PD mechanisms are also quite complicated, since they depend on different physical and chemical parameters. However, the PD measurement should be reflected in their physics and then in their current pulse waveforms. The reason is that the rise and fall times of a PD current pulse waveform are directly determined by electron avalanche and/or streamer/leader discharge extension, and by diffusion and recombination of charge carriers, etc. [5].

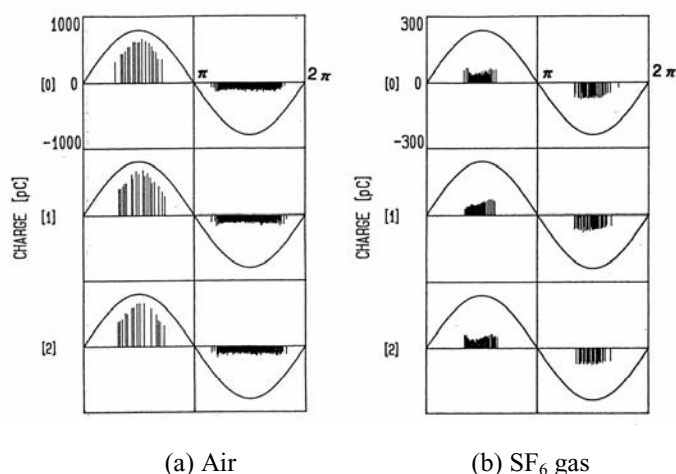
From the above viewpoints, we have been investigating PD characteristics and mechanisms of different insulating materials such as gases, liquids and solids. As an effective tool

to discuss PD mechanisms based on physics, in this paper, we developed a useful PD measurement and analysis technique referred to as "PD Current Pulse Waveform Analysis (PD-CPWA)". PD-CPWA can obtain not only individual PD current pulse waveforms with the time resolution of the order of sub-nanoseconds, but also its time transition from PD inception to BD, with the PD detection sensitivity of 0.1 pC. The obtained PD current pulse waveforms can also be analyzed in terms of different parameters such as peak value, di/dt, rise time, fall time of a single PD pulse, time interval of subsequent PD pulses and so on. This paper introduces the concept, principle and applications of PD-CPWA to PD characteristics in solid, liquid and gas media under ac voltage application.

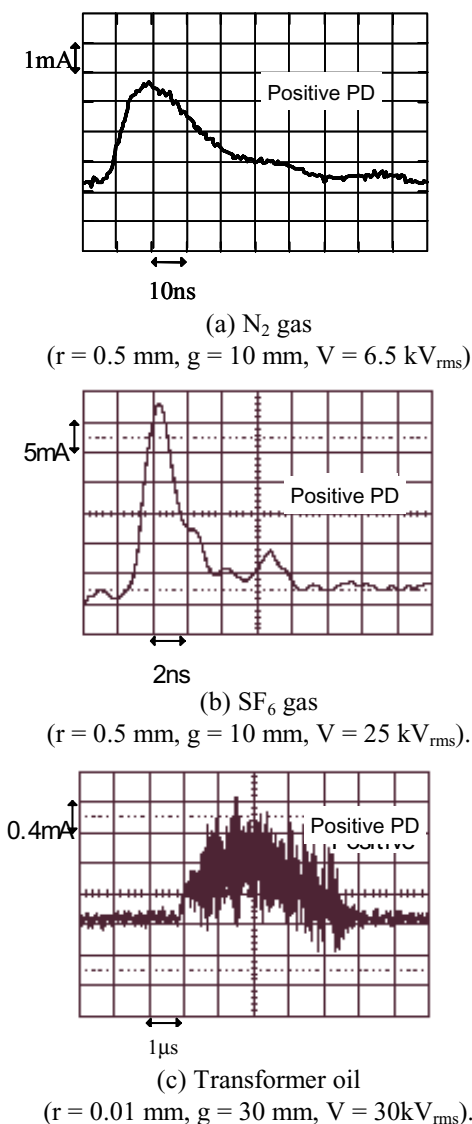
## 2 CONCEPT AND PRINCIPLE OF PD-CPWA

### 2.1 BASIC CONCEPT

Figure 1 shows typical phase-resolved PD characteristics ( $\phi$ -q characteristics) of (a) air and (b) SF<sub>6</sub> gas, respectively, for a needle-plane electrode system. Such phase-resolved PD characteristics allow us to discuss statistical PD characteristics and have contributed to identify the type of defects in the insulating media from the viewpoint of the pattern recognition technique.



(a) Air (b) SF<sub>6</sub> gas  
**Figure 1.** Phase-resolved PD characteristics of air and SF<sub>6</sub> gas for a needle-plane electrode system. ( $r = 0.03$  mm,  $g = 15$  mm,  $V = 5$  kV<sub>rms</sub>).



(a) N<sub>2</sub> gas ( $r = 0.5$  mm,  $g = 10$  mm,  $V = 6.5$  kV<sub>rms</sub>)  
 (b) SF<sub>6</sub> gas ( $r = 0.5$  mm,  $g = 10$  mm,  $V = 25$  kV<sub>rms</sub>)  
 (c) Transformer oil ( $r = 0.01$  mm,  $g = 30$  mm,  $V = 30$  kV<sub>rms</sub>)  
**Figure 2.** PD current pulse waveforms in N<sub>2</sub> gas, SF<sub>6</sub> gas and transformer oil for a needle-plane electrode system.

However, in order to elucidate physical mechanisms of PD inception and propagation, the individual PD current pulse should be discussed in detail [6]. Time-resolved PD characteristics, i.e. PD current pulse waveform as shown in Figure 2 for (a) N<sub>2</sub> gas, (b) SF<sub>6</sub> gas and (c) transformer oil, respectively, will give us much more information based on the physical PD mechanisms. In other words, PD current pulse waveforms may tell us their physics.

## 2.2 KEY TECHNOLOGIES

In order to discuss PD inception and propagation mechanisms leading to BD, we need to obtain sequential characteristics of PD current pulse waveforms during long time duration. Long time measurements of PD current pulse waveforms during seconds, minutes, hours, sometimes days and weeks, with very high time resolution like sub-nanoseconds are required to be developed. After the data acquisition, we need to analyze the numerous data relating to the huge number of generating PD current pulse waveforms, by using computers.

Now, we developed PD-CPWA techniques under the combination of high-speed, high-sensitivity PD measurement and computer application.

The key technologies of PD-CPWA are as follows:

### 2.2.1 PRECISE MEASUREMENT OF PD CURRENT PULSE WAVEFORM

- Simple measuring system using 50 Ω resistor with low leakage inductance and low stray capacitance
- High-speed digital oscilloscope with analog band width of 2-4 GHz and sampling rate of 15-20 GS/s
- Noise reduction with shielding and earth techniques, etc.

The establishment of PD measuring system with the detection sensitivity in the charge magnitude as small as 0.1 pC and the reproducibility of PD current pulse waveform with the rise time as short as 200-300 picoseconds is the prerequisite condition of PD-CPWA.

### 2.2.2 LONG TIME MEASUREMENT OF PD CURRENT PULSE WAVEFORM

- Digital oscilloscope with the memory as long as 32-64 MWord for PD measurement up to the order of milliseconds
- Switch-over of digital oscilloscopes using high-frequency switching technique for PD measurement from the order of milliseconds to hours or days
- Memory saving by successive PD measurements only when PD current pulses were detected
- Data compression and high-speed data transmission

Thousands of PD current pulse waveforms together with the time resolution of the order of sub-nanoseconds as described in (a) are necessary to be recorded in the digital oscilloscope.

### 2.2.3 COMPUTER-AIDED ANALYSIS OF PD PARAMETERS

- Extraction of different parameters on PD current pulse waveform such as peak value  $I$ ,  $di/dt$ , rise time  $t_r$ , fall time  $t_f$  of a single PD current pulse waveform as illustrated in Figure 3, and time interval  $\Delta t$  of

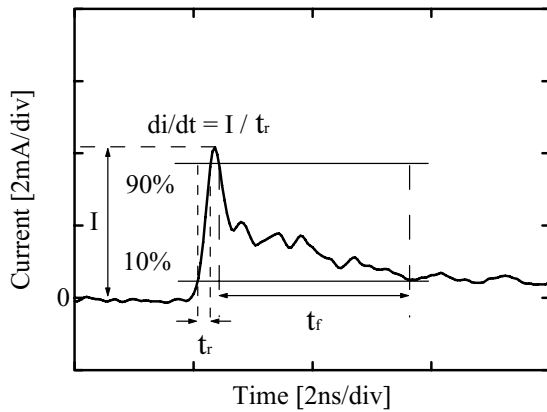


**Figure 3.** Definition of peak value  $I$ ,  $di/dt$ , rise time  $t_r$  and fall time  $t_f$  of a single PD current pulse waveform.

subsequent PD pulses, etc.

- Conversion from extracted PD parameters to other physical data such as charge magnitude  $q$ , injected energy  $J$ , frequency-domain analysis FFT, etc.
- Automatic data analysis and pursuit of the time transition for thousands of PD current pulse waveforms

Construction of the database on PD current pulse waveforms is needed to distinguish harmful PD which may cause material degradation leading to BD from the other harmless PD which can be kept watching or ignored, and to identify the promising PD parameters for BD prediction

### 2.3 SYSTEM CONSTRUCTION

Based on the basic concept and key technologies described in the previous sub-sections, we constructed PD-CPWA as schematically illustrated in Figure 4. The PD current pulse signal is converted into the voltage signal through  $50\ \Omega$  resistor as the detecting and matching impedance under the test sample, and fed into a digital oscilloscope (2-4 GHz, 15-20 GS/s, 32-64 MWord). Together with the noise reduction techniques, even a quite small PD signal with the charge magnitude as low as 0.1 pC and the rise time as short as 200-300 picoseconds, such as PD pulses in  $SF_6$  gas, can be detected.

Once the oscilloscope is triggered, PD signal is measured within a preset time duration using the FastFrame function of the oscilloscope. Owing to the long memory of the oscilloscope, more than 6,000-10,000 signals of PD current pulse waveforms can be recorded together with their acquisition times. The applied ac voltage signal is also used as the reference signal in order to identify the generating time and phase angle of the corresponding PD signals. As the result, we can obtain the PD signals with highly compressed and memory saving data.

Each PD current pulse waveform obtained above is saved in the oscilloscope and converted into a data file through GPIB controlled by a personal computer. Then, a series of data files are transmitted to the personal computer through LAN. Using 2 sets of oscilloscopes and personal computers to be flexibly switched over by a high-frequency switch, we can continue to obtain both PD current pulse waveforms and sequential PD generation characteristics without any time restriction from PD inception to BD.

Now, we can reproduce the sequential PD generation characteristics with each PD current pulse waveform in the personal computer. Then, the PD signals can be analyzed in terms of different parameters not only for a single PD current pulse waveform but also for its time transition, which will be utilized to understand the PD characteristics and elucidate the PD mechanisms.

Figures 5 and 6 show the time transitions of PD current pulse waveform and rise time, respectively, for an epoxy spacer with thermal ageing, as a typical application of PD-CPWA technique. The test sample was broken down at 33 seconds after the PD inception. The time axis in Figure 5 is successively expanded from the order of seconds (Figure 5a) to nanoseconds before BD (Figure 5c), where the drastic increase in PD magnitude before BD and the last PD leading to BD could be clarified. The time transition of peak value of PD current pulse waveform in Figure 5a was not consistent with that of rise time in Figure 6, which suggests that there could exist the difference in physics between the time transitions of peak current and rise time in the PD current pulse waveform.

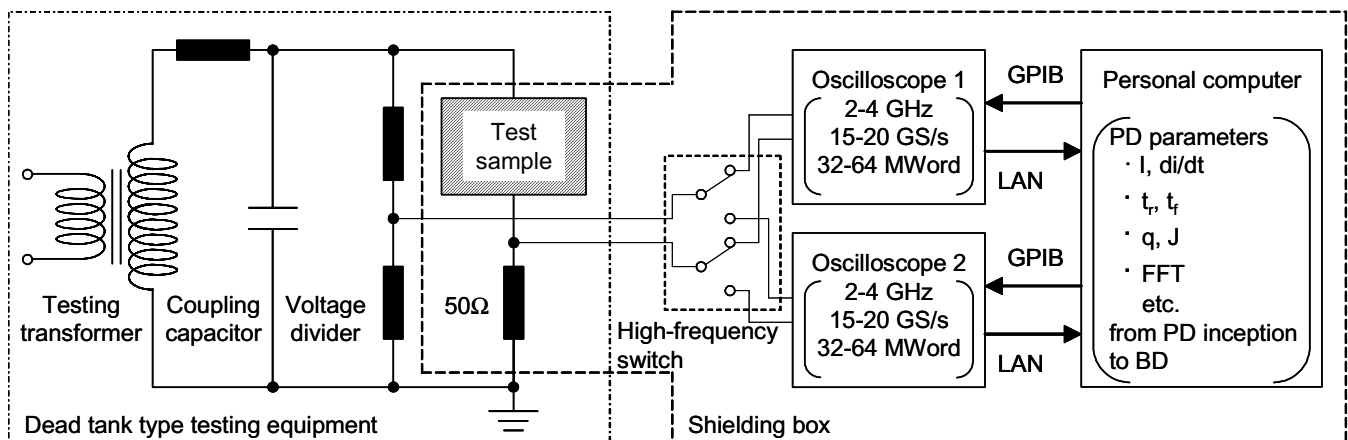
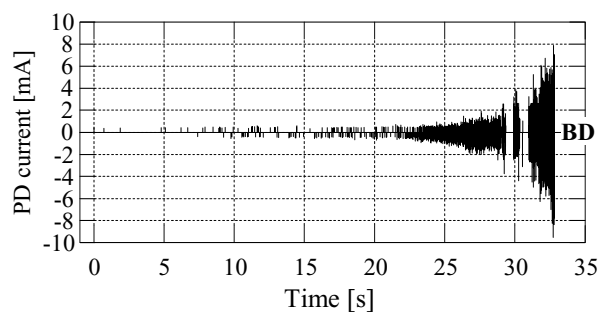
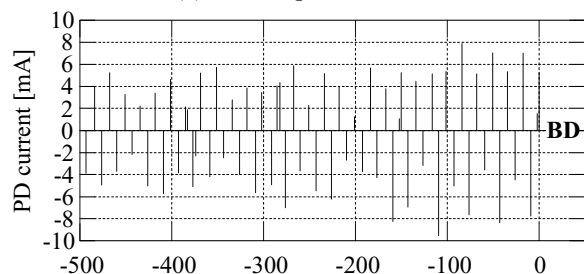


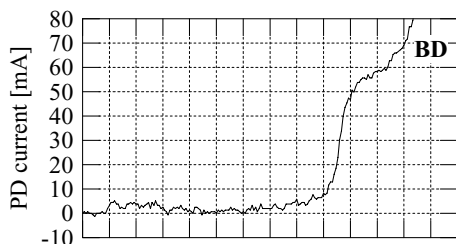
**Figure 4.** Schematic illustration of construction of PD-CPWA technique.



(a) PD inception to BD



(b) Last 500 ms before BD



(c) Last PD leading to BD

**Figure 5.** Time transition of PD current pulse waveform for an epoxy spacer sample with thermal ageing by PD-CPWA technique.

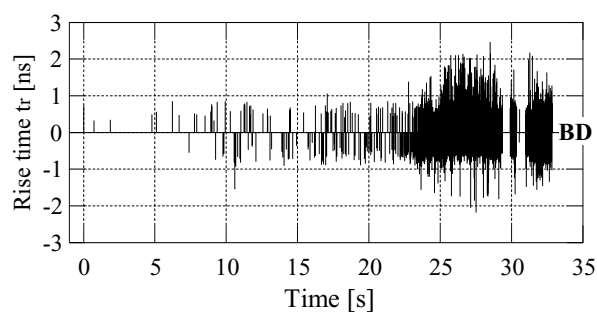


**Figure 6.** Time transition of rise time of PD current pulse waveform for an epoxy spacer sample with thermal ageing by PD-CPWA technique.

### 3 APPLICATION OF PD-CPWA

#### 3.1 PD IN SOLID DIELECTRICS

##### 3.1.1 EXPERIMENTAL SETUP AND PROCEDURE

Application of PD-CPWA to PD in an epoxy spacer for GIS is introduced. Figure 7 shows the experimental setup of an epoxy spacer model [7]. High-voltage and grounded electrodes

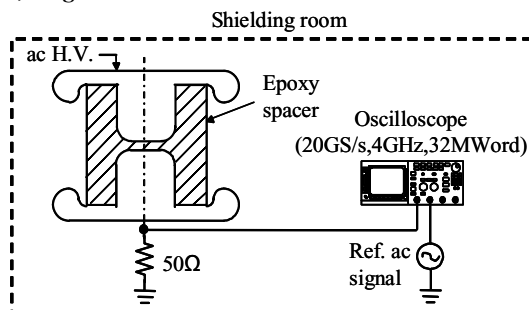


**Figure 7.** Experimental setup of epoxy spacer model.

**Table 1.** Thermal stress condition of epoxy spacer samples.

Temperature [°C]	Heating duration [hour]	PDIV [kV <sub>rms</sub> ]	Time to BD <sub>t<sub>BD</sub></sub>	Number of PD pulses from PD inception to BD	
				Negative	Positive
105	40	125.2	2min 26s	60	1
140	40	122.4	12min 22s	12194	17336
150	15	150.7	33s	697	737
160	1	153.6	1min 55s	191	143
		150.4	1.7s	90	38
		147.4	4.7s	248	114
	5	114.4	> 3hours	-	-
180	1	136.4	10s	437	382
	5	141.0	11min 22s	3340	2026

made of aluminum with the edge radius of 6 mm were embedded in the epoxy resin. The gap length between both the electrodes was 4 mm. The virgin sample of the epoxy spacer model was PD free up to 154 kV<sub>rms</sub> under ac 60 Hz voltage application.

Simulating the operational condition of GIS, thermal stress was applied to the epoxy spacer models in an oven for different temperatures and durations. Table 1 summarizes the thermal stress conditions for total 9 samples. Each sample was placed in SF<sub>6</sub> gas at 0.4 MPa. Then, electric stress was applied to the sample and generated PD. After the PD inception, the applied voltage was kept at the PD inception voltage (PDIV). The sequential PD generation characteristics were obtained by PD-CPWA from PD inception to BD.

#### 3.1.2 EXPERIMENTAL RESULTS

Figure 8 shows PD generation characteristics from PD inception to BD for the sample with thermal stress of 180 °C for 5 h. PDIV was 141.0 kV<sub>rms</sub> and BD was induced at 11 minutes 22 seconds after the PD inception. Total 5,366 PD pulses (positive: 3,340, negative: 2,026) were generated from PD inception to BD. Such statistical data of PD generation characteristics for each sample are shown in Table 1.

Figures 9a to 9g show the time transitions of PD parameters analyzed by PD-CPWA for the last 60 s before BD in Figure 8: (a) peak value I with their waveforms, (b) di/dt, (c) rise time t<sub>r</sub>, (d) fall time t<sub>f</sub>, (e) PD charge q, (f) PD energy J of each PD current pulse waveform, respectively, and (g) accumulated PD energy J<sub>a</sub>. q was calculated by the integration of PD current pulse waveform, and J was evaluated by the product of PD charge and applied voltage. The following tendencies can be derived from Figure 9:

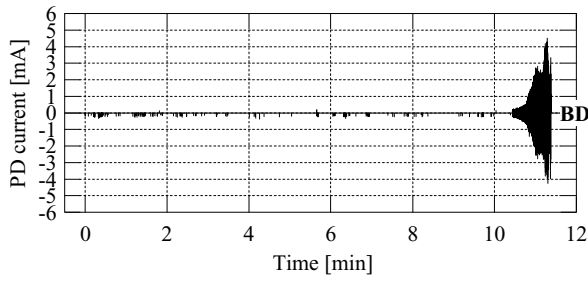


Figure 8. PD-CPWA application from PD inception to BD for epoxy spacer sample with thermal ageing of 180 °C for 5 h.

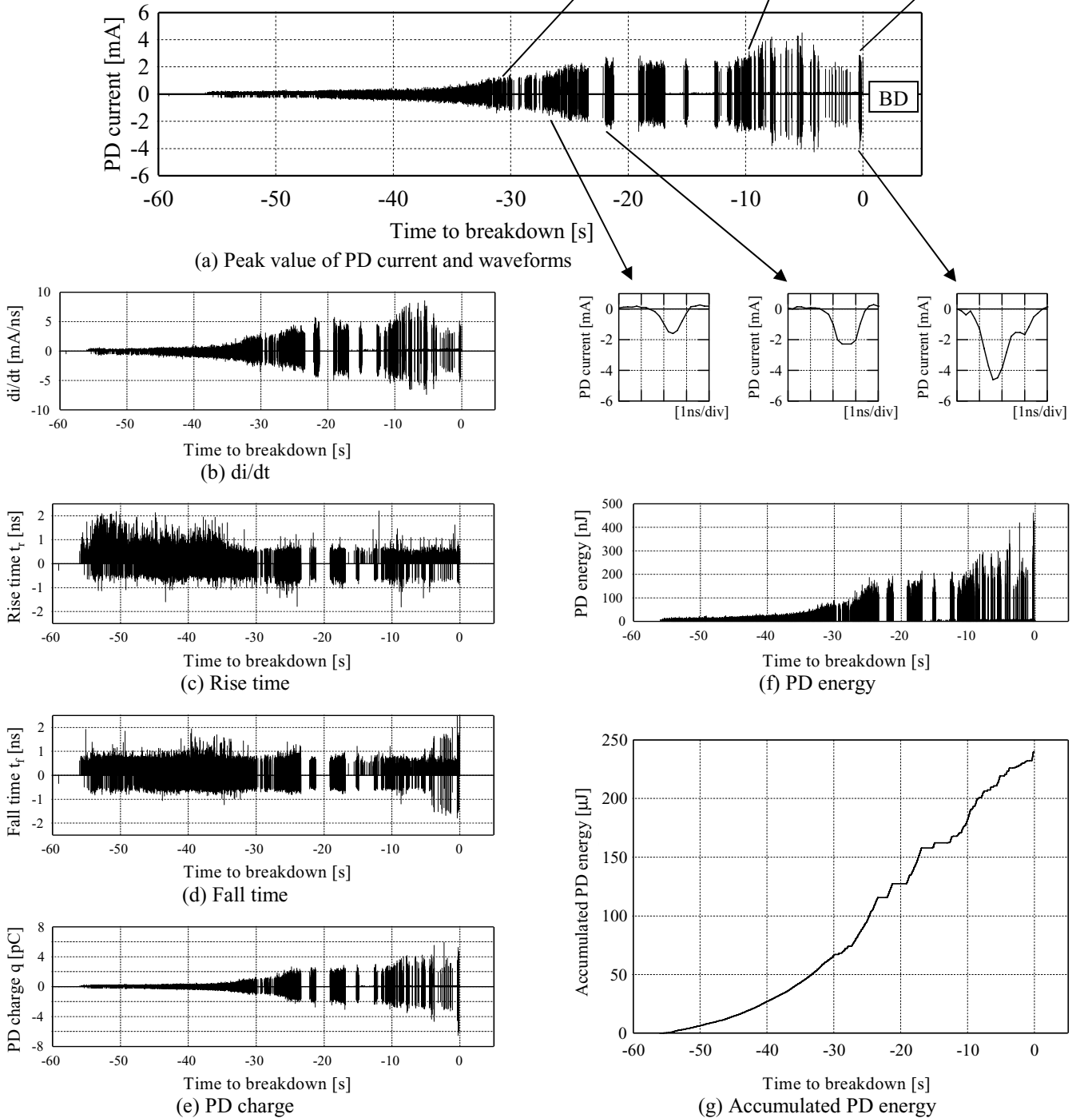
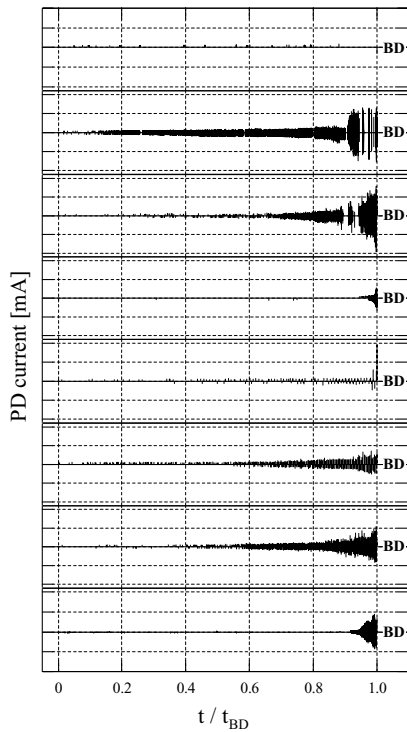


Figure 9. PD-CPWA application for the last 60 seconds before BD for epoxy spacer sample with thermal ageing of 180 °C for 5 h.

- (1) PD current pulse waveform becomes larger and steeper with the elapse of time.
- (2) PD generation was not continuous, but intermittent from PD inception to BD.
- (3) Time transitions of  $di/dt$ ,  $q$  and  $J$  were almost consistent with that of peak value  $I$ .
- (4) Time transitions of  $t_r$  and  $t_f$  were not consistent with that of peak value  $I$ .
- (5) Polarity difference in each PD parameter was not significant.
- (6) Accumulated PD energy  $J_a$  gradually increased and reached about 240  $\mu\text{J}$ , in this sample, just before BD.

3.1.3 DISCUSSIONS

The above PD generation characteristics have a certain tendency to BD in most samples, irrespective of the difference in thermal stress conditions. Figures 10 and 11 show the time transition of  $I$  and  $di/dt$  for 8 samples resulted in BD within 3 hours, respectively, where PDIV, time to BD and number of PD pulses for each sample are listed in Table 1. Figure 12 shows the time transition of time interval  $\Delta t$  of subsequent PD pulses for 4 samples. Note that the horizontal time axes in Figs. 10, 11 and 12 are normalized by the time to BD after PD inception in each sample. The drastic increase in  $I$  and  $di/dt$  before BD was also consistent with the decrease in  $\Delta t$  into the order of microseconds.



- (a) 105 °C for 40 hours  
PDIV=125.2 kV<sub>rms</sub>
- (b) 140 °C for 40 hours  
PDIV=122.4 kV<sub>rms</sub>
- (c) 150 °C for 15 hours  
PDIV=150.7 kV<sub>rms</sub>
- (d) 160 °C for 1 hour  
PDIV=153.6 kV<sub>rms</sub>
- (e) 160 °C for 1 hour  
PDIV=150.4 kV<sub>rms</sub>
- (f) 160 °C for 1 hour  
PDIV=147.4 kV<sub>rms</sub>
- (g) 180 °C for 1 hour  
PDIV=136.4 kV<sub>rms</sub>
- (h) 180 °C for 5 hours  
PDIV=141.0 kV<sub>rms</sub>

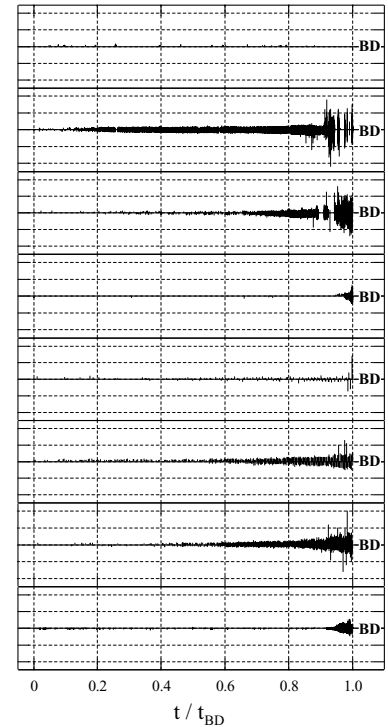


Figure 11. Time transition of steepness  $di/dt$  for 8 epoxy spacer samples resulted in BD.

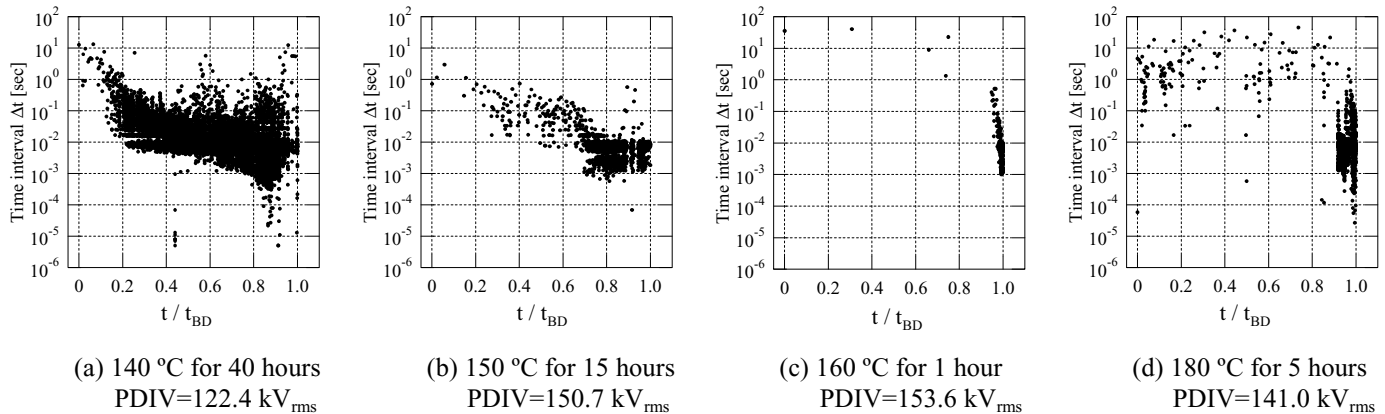


Figure 12. Time transition of time interval  $\Delta t$  of sequent PD pulses for 4 epoxy spacer samples resulted in BD.

Such time transition of PD parameters may be attributed to the change of physical properties of the epoxy resin under the thermal and electric field stresses. The insulation performance of epoxy resin would be deteriorated due to electron impact, local temperature rise, chemical reaction and so on at the interface between the epoxy resin and the embedded electrode. The insulation degradation of the epoxy resin could further activate the PD development in the epoxy resin. Such a positive feedback process between the PD generation and the insulation degradation of epoxy resin would be accumulated during the long time voltage application and result in BD when a specific PD parameter reached the critical level.

PD-CPWA is expected to contribute to identify the specific PD parameter to be closely related to the physical mechanisms of insulation degradation leading to BD in epoxy spacer for GIS. PD-CPWA can also be applied to the PD measurement and analysis for XLPE cables.

### 3.2 CREEPAGE PD IN SF<sub>6</sub> GAS

#### 3.2.1 EXPERIMENTAL SETUP AND PROCEDURE

Figure 13 shows the experimental setup for creepage PD measurement in SF<sub>6</sub> gas [8]. A needle was fixed on an epoxy plate between parallel plane electrodes in SF<sub>6</sub> gas at 0.1 MPa (dimensions are shown in Figure 13). In order to measure PD current pulse waveform generating at the needle tip under ac 60 Hz voltage application, a detecting and matching circuit with 50 Ω resistor was set under the epoxy plate. The detected PD signals were fed into the digital oscilloscope and analyzed by PD-CPWA. In addition, PD light emission image was also observed by a digital camera through an image intensifier.

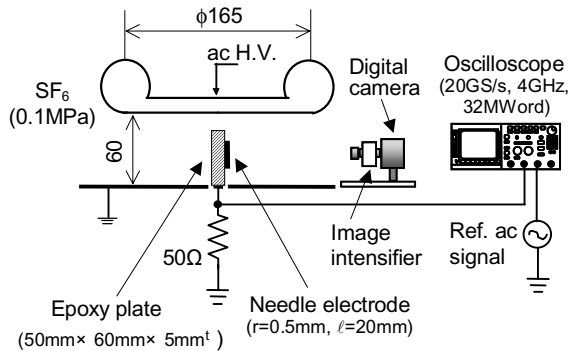


Figure 13. Experimental setup of needle on epoxy plate.

Table 2. Arrangement of needle and epoxy plate.

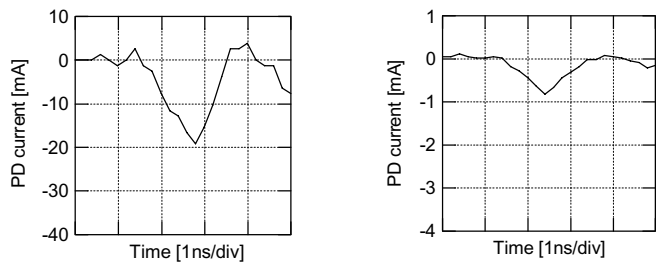
Electrode arrangement	ac H.V. / SF <sub>6</sub> / Needle	ac H.V. / SF <sub>6</sub> / Needle	ac H.V. / SF <sub>6</sub> / Needle	ac H.V. / SF <sub>6</sub> / Needle
	Needle on grounded electrode	Fixed needle on middle of epoxy plate	Fixed needle on grounded electrode with epoxy	Fixed needle on high voltage electrode with epoxy
PDIV [kV <sub>rms</sub> ]	19.0	22.5	12.5	12.2
Applied voltage [kV <sub>rms</sub> ]	30.0	35.0	20.0	20.0

Table 2 shows different arrangements of needle and epoxy plate with the measured PDIV. When PD-CPWA was applied to each arrangement, the applied voltage was set at about 160 % of PDIV, because the number of PD signals to be shown later decreased with the elapse of time. PD measurement under PD-CPWA was repeated in every 2 minutes for 30 minutes.

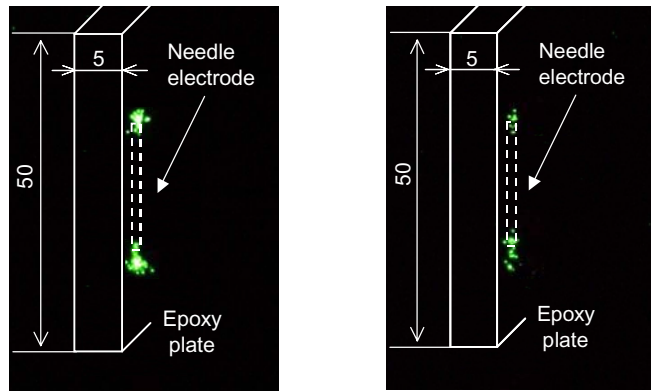
#### 3.2.2 EXPERIMENTAL RESULTS AND DISCUSSIONS

Figure 14 shows (i) typical PD current pulse waveforms in the negative cycle and (ii) PD light emission images for 1 s, respectively, at (a) t = 0 min and (b) t = 30 min after the voltage application, when the needle was fixed on the middle of epoxy plate. The peak value of PD current pulse waveform at t = 30 min decreased drastically into 1/20 of that at t = 0 min. Such a relaxation of PD activity can also be verified by the PD light emission images, where the PD light intensity at both ends of the needle at t = 0 min was much higher than that at t = 30 min. On the other hand, the rise time and fall time in the PD current pulse waveform at t=0 min were nearly equal to those at t = 30 min, respectively, which means that di/dt decreased with the elapse of time.

Figure 15 shows the time transition of averaged values and standard deviations of positive and negative PD current pulses in every 2 minutes, when the needle was fixed on the middle of epoxy plate. The averaged values of PD current pulses decreased drastically within the first 2 minutes and then gradually decreased or almost constant after 2 minutes. Figure 16 shows the time transition of di/dt in the negative cycle for different arrangements in Table 2. Note that di/dt in Figure 16 are normalized by those just after the voltage application. The



(i) PD current pulse waveform



(ii) PD light emission image

(a) t=0 min

(b) t=30 min

Figure 14. Time transition of PD current pulse waveform and PD light emission image for creepage PD.

time transition of  $di/dt$  depended on the location of the needle fixed on the epoxy plate. The time constants of the decrease in  $di/dt$  were about 1, 2 and 5 minutes, respectively. The difference in the time constant will be interpreted by the charging characteristics and mechanisms on the epoxy plate as well as the resultant distortion of electric field distribution for each arrangement.

The above measurement and discussion on the transition of PD parameters using PD-CPWA can contribute to locate the fixed particles on epoxy spacer and distinguish them from free particles in GIS.

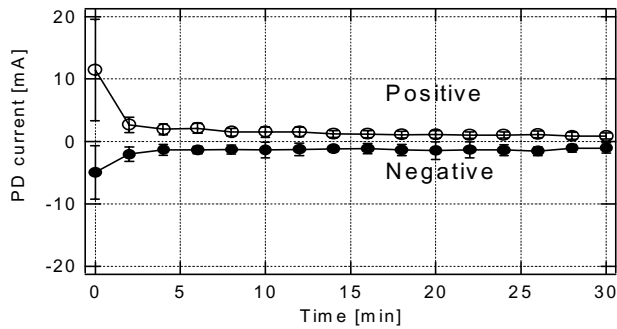


Figure 15. Time transition of peak value of PD current pulse waveform for creepage PD.

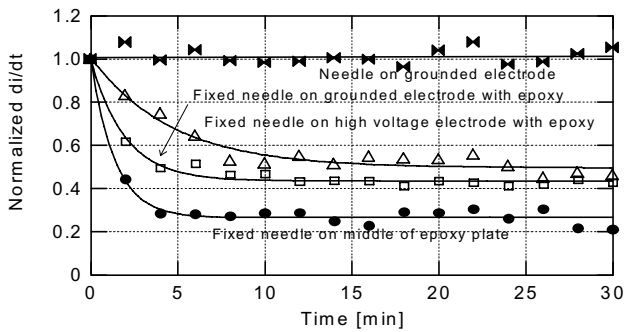


Figure 16. Time transition of steepness  $di/dt$  of PD current pulse waveform for creepage PD.

### 3.3 PD IN LIQUID/SOLID COMPOSITE SYSTEM

#### 3.3.1 EXPERIMENTAL SETUP AND PROCEDURE

Another application of PD-CPWA to PD in liquid/solid composite system is introduced. Figure 17 shows the experimental setup of liquid nitrogen / polypropylene laminated paper composite insulation system for high temperature superconducting cables [9]. A coaxial cylindrical cable model with the insulation thickness of 1 mm (0.125 mm x 8 layers) and the effective length of 150 mm was immersed in liquid nitrogen at 77 K. In the similar way as those in the previous sub-sections, PD current pulse waveform under ac 60 Hz voltage application was measured through 50  $\Omega$  resistor and analyzed by PD-CPWA.

#### 3.3.2 EXPERIMENTAL RESULTS AND DISCUSSIONS

PDIV of the cable model was 18 kV<sub>rms</sub> and BD was induced at 35 kV<sub>rms</sub>. Figure 18 shows the time transitions of peak value of PD current pulse waveform at the applied voltage of (a) 20 kV<sub>rms</sub>, (b) 26 kV<sub>rms</sub> and (c) 35 kV<sub>rms</sub>, respectively. The peak value and number of PD pulses per second increased with the

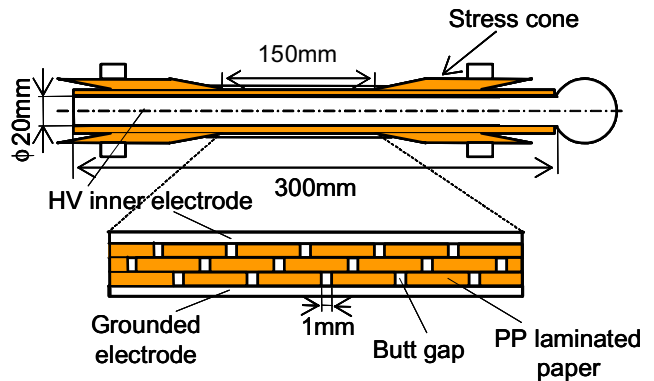


Figure 17. Experimental setup of LN<sub>2</sub>/PP laminated paper composite insulation system.

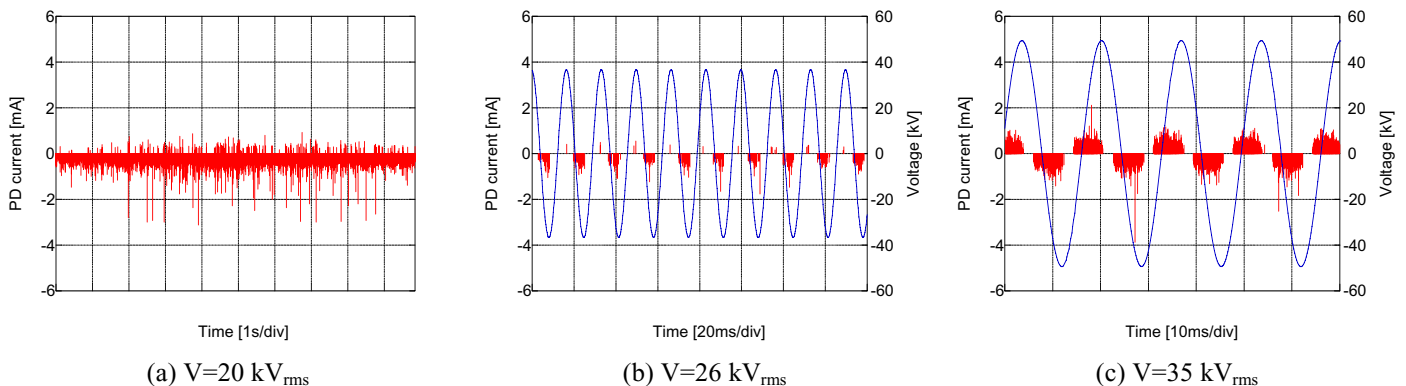
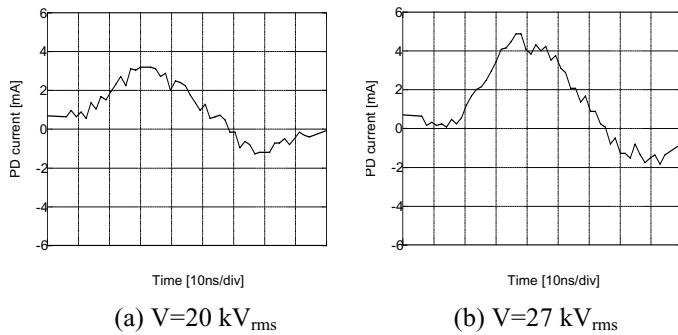


Figure 18. Time transition of peak value of PD current pulse waveform for LN<sub>2</sub>/PP laminated paper composite system.



**Figure 19.** PD current pulse waveform in LN<sub>2</sub>/PP laminated paper composite insulation system.

applied voltage. PD pulses at the lower applied voltage were generated at around the peak of the applied voltage, whereas those at the higher applied voltage also appeared at around the zero-crossings. These results suggested that the PD generation mechanisms changed into void-like discharges not only in butt gaps but also in the other micro gaps between the laminated paper layers [9].

Figure 19 shows typical PD current pulse waveforms at the applied voltage of (a) 20 kV<sub>rms</sub> and (b) 27 kV<sub>rms</sub>, respectively. The averaged values of rise time and fall time in PD current pulse waveform were about 18 ns and di/dt was about 0.02 mA/ns, irrespective of the applied voltage. These values were longer and slower than those of the epoxy spacer and creepage PD in SF<sub>6</sub> gas in the previous sub-sections. Even the outstanding large PD pulses in a cluster of small PD pulses in Figure 18c had the similar rise time, i.e. steeper di/dt, compared with those in the cluster. Such a contamination of large PD pulses suggests the superposition of PD pulses with different PD mechanisms from that of void-like discharges. By analyzing the PD parameters, we will be able to identify the PD location in butt gaps or laminated paper layers and liquid or gas phase, etc.

As described above, PD-CPWA was verified to contribute to discuss the change of PD generation characteristics and their physical mechanisms for different electrical insulating materials and circumstances.

## 4 CONCLUSIONS

PD measuring technique with understanding discharge mechanisms should be developed in order to establish the reliable insulation diagnosis of high-voltage power apparatus. We developed “PD Current Pulse Waveform Analysis”, abbreviated to “PD-CPWA”, focusing on PD current pulse waveform including different physical processes on discharge inception, propagation and breakdown. The concept, principle and applications of PD-CPWA were introduced in this paper. PD-CPWA is expected to have a wide variety of application to different electrical insulating materials such as gas, liquid, solid, vacuum and their composite insulation systems.

## REFERENCES

- [1] S. Boggs and J. Densley, “Fundamentals of Partial Discharge in the Context of Field Cable Testing”, IEEE Electr. Insul. Mag., Vol.16, No.5, pp.13-18, 2000.
- [2] O. Farish, “Breakdown in SF<sub>6</sub> and its Mixtures in Uniform and Nonuniform Fields”, Intern. Sympos. Gaseous Dielectrics I, pp.60-83, 1978.
- [3] F. Pinnekamp and L. Niemeyer, “Qualitative Model of Breakdown in SF<sub>6</sub> in Inhomogeneous Gaps”, J. Phys. D: Appl. Phys., Vol.16, pp.1293-1302, 1983.
- [4] R. Baumgartner, B. Fruth, W. Lanz and K. Pettersson, “Partial Discharge – Part X: PD in Gas-Insulated Substations – Measurement and Practical Considerations”, IEEE Electr. Insul. Mag., Vol.8, No.1, pp.16-27, 1992.
- [5] H. Okubo, N. Hayakawa and A. Matsushita, “The Relationship Between partial Discharge Current Pulse Waveforms and Physical Mechanisms”, IEEE Electr. Insul. Mag., Vol.18, No.3, pp.38-45, 2002.
- [6] H. Okubo, A. Suzuki, T. Kato, N. Hayakawa and M. Hikita, “Frequency Component of Current Pulse Waveform in Partial Discharge Measurement”, 9th Intern. Sympos. High Voltage Engineering, No. 5634, 1995.
- [7] H. Okubo, S. Watanabe, N. Hayakawa and T. Kumai, “Insulation degradation Mechanism of Epoxy Spacer Samples for GIS”, Intern. Sympos. Gaseous Dielectrics X, pp.353-360, 2004.
- [8] H. Okubo, Y. Okamoto, N. Hayakawa, T. Hoshino and S. Matsumoto, “Partial Discharge Characteristics by Metallic Particle on Solid Insulator in GIS”, 13th Intern. Sympos. High Voltage Engineering, p.332, 2003.
- [9] N. Hayakawa, M. Nagino, H. Kojima, M. Goto, T. Takahashi, K. Yasuda and H. Okubo, “Dielectric Characteristics of HTS Cables Based on Partial Discharge Measurement”, Applied Superconductivity Conference, 1LT04, 2004.



**H. Okubo** (M’81) was born on 29 October 1948. He received the Ph.D. degree in 1984 in electrical engineering from Nagoya University. He joined Toshiba Corporation/Japan in 1973 and was a manager of the high voltage laboratory of Toshiba. From 1976 to 1978, he was at the RWTH Aachen/Germany and the TU Munich/Germany. In 1989, he became an Associate Professor of Nagoya University at the Department of

Electrical Engineering and presently he is a Professor of Nagoya University at the EcoTopia Science Institute. He is a member of IEE of Japan, VDE and CIGRE.



**N. Hayakawa** (M’90) was born on 9 September 1962. He received the Ph.D. degree in 1991 in electrical engineering from Nagoya University. Since 1990, he has been at Nagoya University and presently he is an Associate Professor of Nagoya University at the Department of Electrical Engineering and Computer Science. From 2001 to 2002, he was a guest scientist at the Forschungszentrum Karlsruhe/Germany. He is a

member of IEE of Japan.